Iraqi Journal of Physics, 2021 *Vol.19, No.49, PP. 62-74*

DOI: 10.30723/ijp.v19i49.646

Hydrophilic Properties Study of Mn-TiO_2 Thin Films Deposited by Dipping Technique

Sura Y. Khalaf, Falah H. Ali

Department of Physics, College of Science, University of Baghdad

E-mail: falah.ali@scbaghdad.edu.iq

Corresponding author: surakyassen@yahoo.com

Abstract

This work presents the effect of Mn-doping TiO_2 on the optical and structural properties of TiO_2 films synthesized by sol-gel method, and deposited by the dip-coating technique. The characteristics of pure and Mn-doped TiO_2 were studied by X-ray diffraction (XRD), the measurements show the anatase phase for all the thin films. The spectrum of UV-Vis. absorption of increases Mn-TiO_2 concentrations (1%, 3%, 5%, 7%, and 9%) indicates a red shift; therefore, the energy gap decreases with increased of doping. The minimum value of energy gap (2.51 eV) at 7% weight. Scanning electron microscope (SEM) measurement showed that the particles size of thin films decreases with doping and has a minimum value with 7%wt doping ratio. Then self-cleaning test, under UV and visible light was adopted. Hydrophilic properties demonstrate (super hydrophilicity) where θ reaching less than 10˚ in 15 minutes.

Key words

Self-cleaning, sol – gel method, Mn-doped Hydrophilicity property.

Article info.

Received: Nov. 2020
Accepted: Apr. 2021
Published: Jun. 2021

دراسة الخصائص المحبة للماء للأغشية الرقيقة Mn-TiO_2 المرسبة بواسطة جهاز الغمر

سرى ياسين خلف، فلاح حسن علي

قسم الفيزياء, كلية العلوم, جامعة بغداد

الخلاصة

يعرض هذا البحث تاثير التطعيم بالمنغنيز على الخواص البصرية والتركيبية لاغشية الTiO_2 المحضرة بواسطة طريقة السول - جل والمرسبة بواسطة تقنية الطلاء بالغمر. وقد تمت دراسة خصائص كل من TiO_2 النقي والمطعم بالمنغنيز بواسطة قياس حيود الاشعة السينية XRD وتبين ان طور الانتس يظهر في كل الاغشية الرقيقة المحضرة، ويشيرنطاق الامتصاص الى العديد من تراكيز المنغنيز(1%,3% 5,% 7,% و 9%) تؤدي الى ازاحة باتجاه المنطقة الحمراء، وبالتالي، فان فجوة الطاقة تقل مع زيادة تراكيز Mn. ان القيمة الدنيا لفجوة النطاق (2.51eV) عند وزن 7%. وتمت دراسة خصائص الهيكلية للعينات المحضرة باستخدام المجهر الالكتروني الماسح (SEM) وتبين ان الحجم الحبيبي يقل بزيادة نسبة التطعيم، وان اقل حجم حبيبي ظهرعند نسبة التطعيم 7 %. تم اختبار التنظيف الذاتي باستخدام الأشعة فوق البنفسجية والضوء المرئي، حيث أظهر خصائص محبة للماء وزاية التماس تصل إلى θ˚>10 في 15 دقيقة. وهذا جيد في عملية التحفيز الضوئي.

Introduction

In the last four decades, the field of heterogeneous photocatalysis has grown rapidly, having undergone numerous developments, especially in relation to energy and the environment. In the presence of a catalyst, it can be described as the acceleration of photoreaction. [1]. Fujishima and Honda (1972) discovered the photic

splitting of water on TiO_2 electrodes, which has marked the beginning of heterogeneous photocatalysis [2] Since then, enormous research efforts have been made to understand the fundamental process of heterogeneous photocatalysis thus improving the performance of photocatalytic [3, 4]. Titanium dioxide (TiO_2) heterogeneous semiconductor photocatalysis has been extensively investigated for the oxidative degradation of various organic and inorganic contaminants in the air / water environment due to its strong oxidation strength, high photocatalytic degradation capability, chemical and biological stability, low cost, abundance and chemical corrosion stability [2, 5, 6]. Titanium dioxide (TiO_2, Titania) is used widely in several applications, [7], including dye-sensitized solar cells (DSSCs) [8], water and air purification [9], self-cleaning [10]. TiO_2 is an antibacterial and disinfection wide-band semiconductor with an optical indirect band gap for anatase ranging from 3.0 eV to 3.9 eV [11, 12]. The development of self-cleaning materials and an understanding of the relationship between their structure and functions constitute an active field of research, in recent years, due to its broad applications in various fields ranging from interior applications in fabrics, window glasses, exterior construction materials, and bishop tiles, these materials have received great interest [13-16]. These materials easily stream nature water like rain, the self-cleaning activity is predominant in nature, as in the cases of lotus leaves. When the water droplets roll over the leaves, the particles of dust / dirt are removed. This method is known in a wide range by the "lotus effect" [17, 18]. In the case of hydrophilic surfaces, water droplets scatter on the surface and form a layer of water during the diffusion process, the contaminants are washed away on the surface. Self-cleaning surfaces may be split into two parts, hydrophilic surfaces and hydrophobic surfaces. Due to its water-repellent properties and low adhesive surface, the water droplets roll on the surface easily in the case of hydrophobic surfaces and in turn eliminates contaminants [19-21].

Experimental work

1. Materials: Titanium (IV) TetraIsopropoxide (TTIP), Ti [OCH(CH_3)2]4 from Sigma-Aldrich, [purity 97% percent].1-propanol CH_3CH_2OH (assay 99.8%) from GCC. Manganous $MnCL_2$. $4H_2O$, (pure 97%), from GPS, and deionized water.

2. Preparation of pure and Mn - doped TiO_2 Thin film: Preparation of pure TiO_2 and Mn-doping nanoparticles by sol gel method, the particles were precipitated by dip-coating technique, by adding 1.2 ml of TTIP to 1.2 ml of 1- propanol (sol A), then deionized water with pH adjustment by HNO_3 (sol B), sol B was then added to sol A dropwise, The solution was placed on a magnetic stirrer for 4 hours. The resulting solution was aged at 55° C for 24 h [22]. Then calcination was adopted at 500 ˚C to get the largest percentage of anatase phase. The preparation of concentrations (1%, 3%, 5 %, 7 % and 9 %) Mn-doped TiO_2 was similar to that of pure TiO_2, were add to the solution (B), while operation similar to prepped pure TiO_2. Doped-TiO_2 samples were denoted as (TMx), where x represents the grade of doping concentration. The character x can take value of 1, 2, 3, and 4 for the doping concentration of 1%, 3%, 5%, 7% and 9% respectively.

3. Thin film preparation

Before depositing the thin films, first the substrates are cleaned thoroughly in an oven at 400 °C for 15 minutes to remove organic contaminants from them. To precipitate thin films on the glass substrates by immersing the substrates in a solution of TiO_2 (sol), that mentions in above content were prepared at concentrations (1%,

3%, 5%, 7% and 9%) of Mn-TiO_2 using a dip- coating technique, the substrates remained in the sol for one minute, then were withdrawn at a uniform rate at a constant speed (9 mm / s). The substrate was dried in an oven for 10 minutes at 55 °C [23]. Finally, it was dried in an oven for 2 hours at 500 °C for obtain thin films to use as photocatalysts.

4. Contact angle

Fig.1 shows a diagram for contact angle. The photo-induced hydrophilic property was evaluated by measuring the water contact angle of the films using contact angle device, three measurements were taken at different time on the same sample with droplets of a constant volume of (5 µL) of water, this process requires a high-resolution fixed camera working to capture the drops image. A computer to accurately control the droplet size, a computer was use to analyze image data.

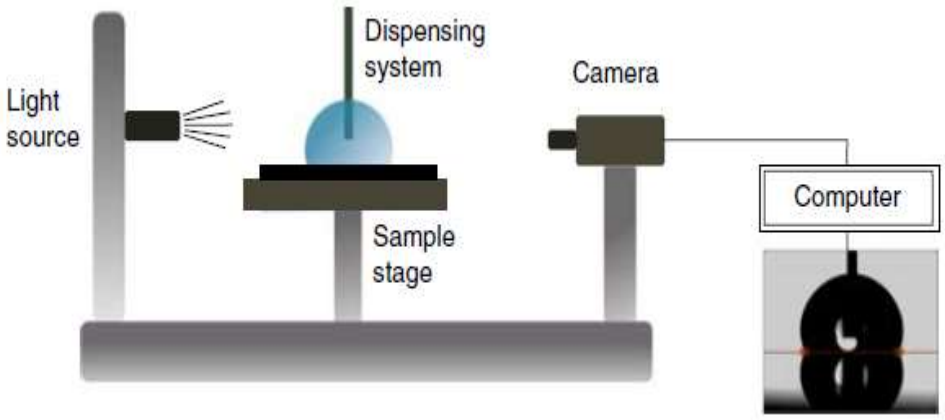

Fig.1: Process of contact angle.

Results and discussion

1. X-ray diffraction

TiO_2 and Mn-doped nanoparticles XRD patterns are shown in Fig.2. XRD was used to analyze the phase structures and crystal size of the prepared thin films. It is shown in TiO_2 pure and Mn-containing samples that the diffraction values of the samples fit well with the anatase diffraction values of the anatase according to the (JCPDS card No 21_1272) reported by Asilturk et al. [24]. The films showed that the crystal level peak diffraction is at (2 Ɵ=25.16) with the crystal level (101), with an increase in the Mn concentration the anatase phase hence remains same. Table 1 shows the sizes of the crystals for all the doped samples Mn. The crystal size is calculated using the Debye– Scherrer equation as shown in Eq.1 and the results show that the smallest crystal size can be obtained at 7% Mn, due to concentration of Mn is increased, then the crystal size becomes smaller.

$$\boldsymbol{D = k\lambda/\beta Cos\theta} \qquad \textbf{(1)}$$

where D is the material's crystallite size (nm), K is the form factor = 0.9, λ is the X-ray wavelength (0.154 nm), β is the radiograph line expanding full width to half maximum intensity (FWHM), θ is angle Bragg's.

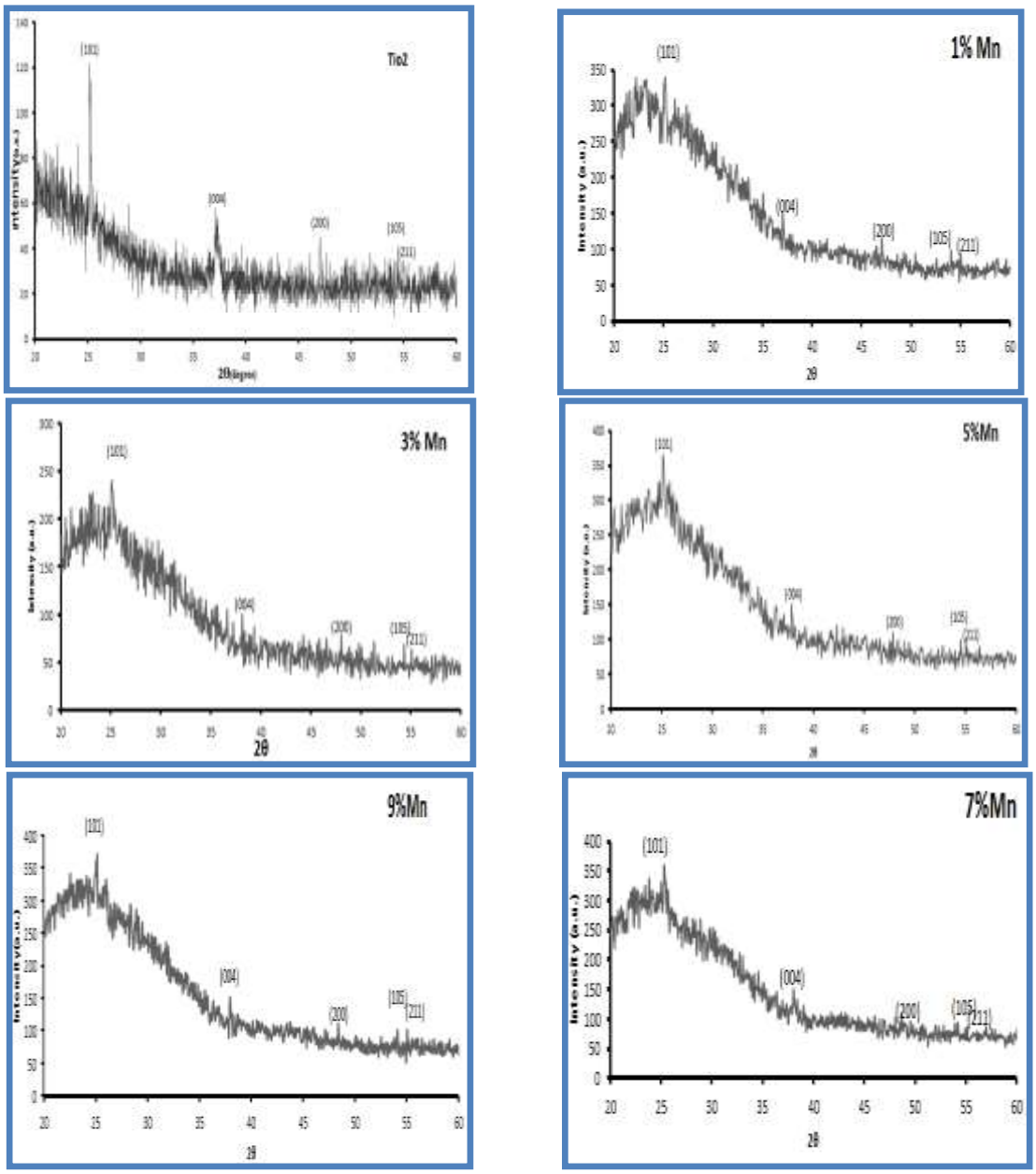

Fig.2: X-ray diffraction of pure and Mn -doped TiO_2 thin film.

Table 1: Summary of the data obtained XRD analysis on the various the prepared Mn-doped TiO2 thin films samples.

Samples	Wt %	2θ degree	FWHM degree	D-crystalline size (nm)	(h k l)	phase
Tm1	1%	25.03	0.5	16.3164	(101)	**anatase**
Tm2	3%	25.13	0.4	20.3994	(101)	**anatase**
Tm3	5%	25.18	0.45	18.1345	(101)	**anatase**
Tm4	7%	25.38	0.81	10.2047	(101)	**anatase**
Tm5	9%	25.08	0.4	20.3994	(101)	**anatase**

2. Scanning Electron Microscopy (SEM)

As the shown Figs.3 and 4 the micrographs obtained by scanning electron microscopy of Mn- doped TiO_2 film ,in 100kx and 50kx of magnification, and scale of (500 nm, 200 nm). As shown in Fig.4 Using image analysis software. The average particle size of (TiO_2) nano particles that is recorded from the image of scale at (200 nm) equal (16.24 nm), which corresponds to the XRD result. The images show that the surface of these films have nanostructures and that the particles are small, uniformly distributed and homogeneous, Thus the surface area increases, and start more homogeneous at a Tm4 where the particle size is 9.36 nm, and the following Table 2 shows the particle sizes for pure TiO_2 and Mn-doped TiO_2 samples.

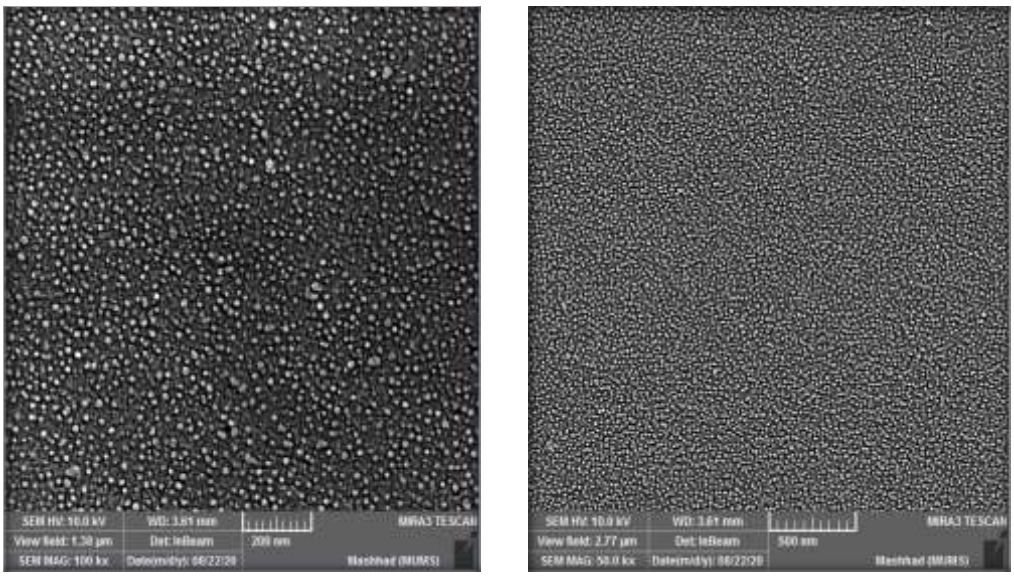

Fig.3: SEM images TiO_2 pure at (200 nm and 500 nm) scale.

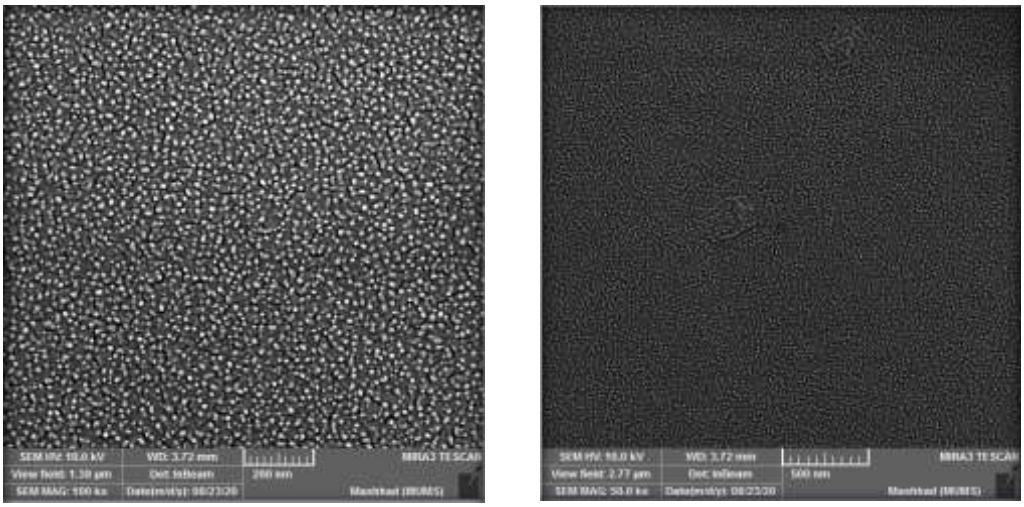

(a) 1% Mn-TiO_2

Fig.4: SEM images of Mn-doped TiO_2 a) 1%.

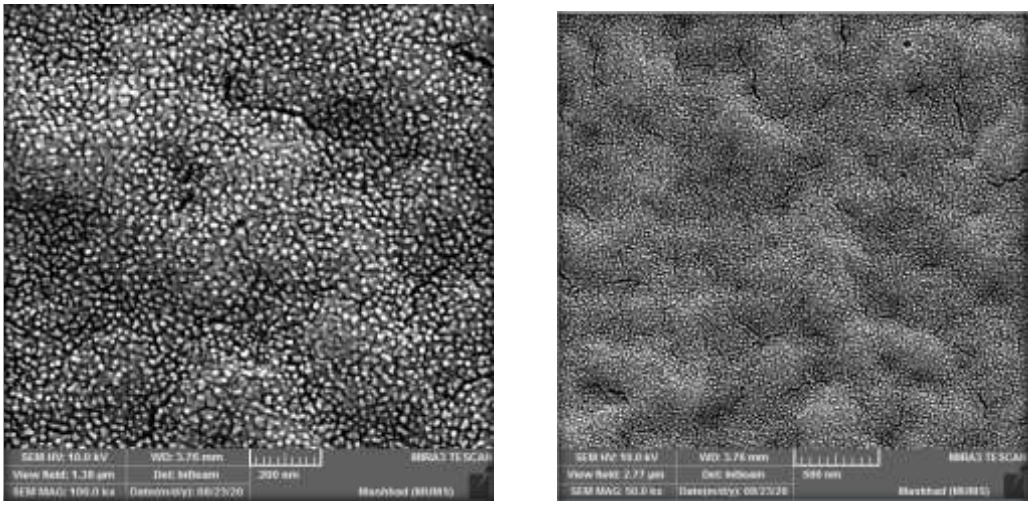

(b) 3% Mn-TiO_2

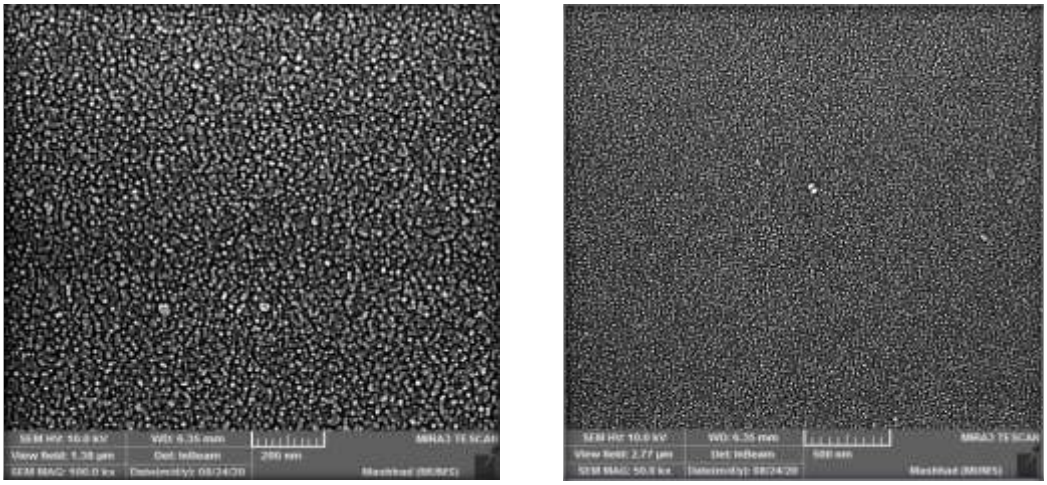

(c) 5% Mn-TiO_2

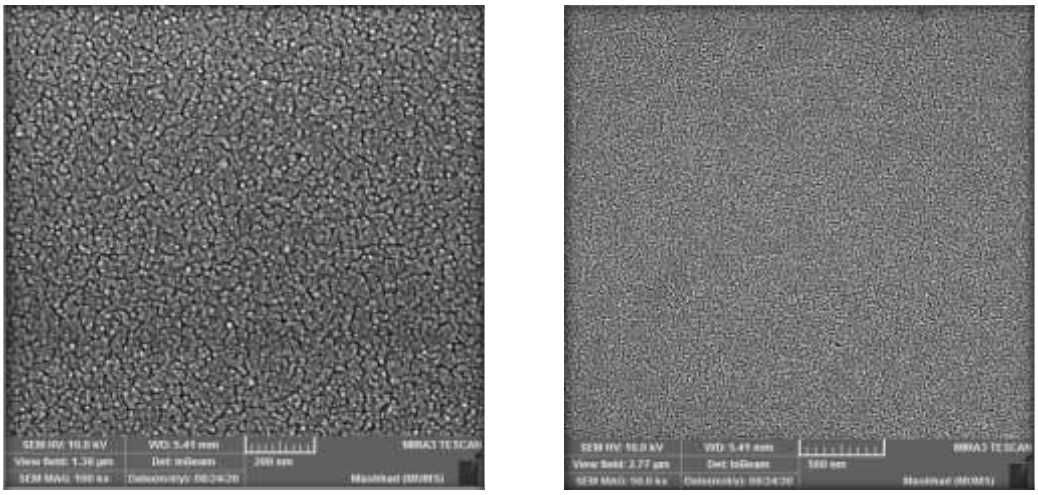

(e) 7% Mn-TiO_2

Fig.4: SEM images of Mn-doped TiO_2 (a 1%, b 3%, c 5%, e 7%).

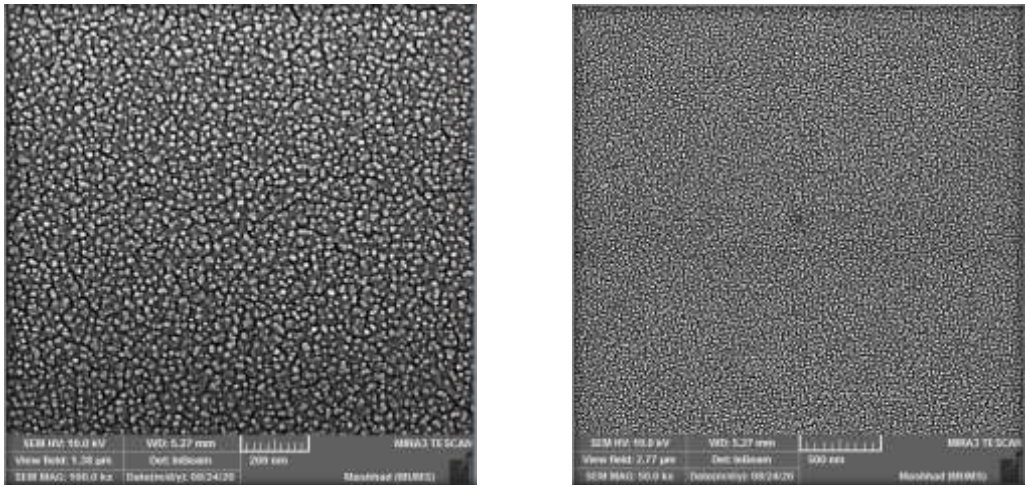

(f) 9% Mn-TiO_2

Fig.4: SEM images of Mn-doped TiO_2 f) 9%.

Table 2: Summary of the data obtained by SEM analysis on the TiO_2 pure and Mn-doped TiO_2.

Samples	Wt %	Average Particle size (nm)
T	0%	16.14
Tm1	1%	11.11
Tm2	3%	11.31
Tm3	5%	11.43
Tm4	7%	9.67
Tm5	9%	15.2

3. UV–Visible spectroscopy

Fig.5 shows a pure TiO_2 UV-Vis. spectral absorption curve with different Mn-doping concentrations was shown. Pure TiO_2 mainly absorbed UV light with a wavelength of less than 390 nm, corresponding to the electronic Arousal from the Valence band the value of the energy gap was 3.2 eV for the of semiconductor conduction band, and the data in the (Table 3) indicate that with increasing manganese the value of the energy gap was 3.2 eV. The absorption edge moved towards the indirect optical lengths (red shift), the band gap decreased as doping increased, the doping level reached 7 %, the optical uptake distribution was clearly over the infrared spectral spectrum, and this is in line with the study. This showed that the red shift in the optical absorption of Ti ions by Mn ions in the TiO_2 matrix properties has been replaced and generally decreases the band gap [25], and this is ideal for photo-catalytic applications.

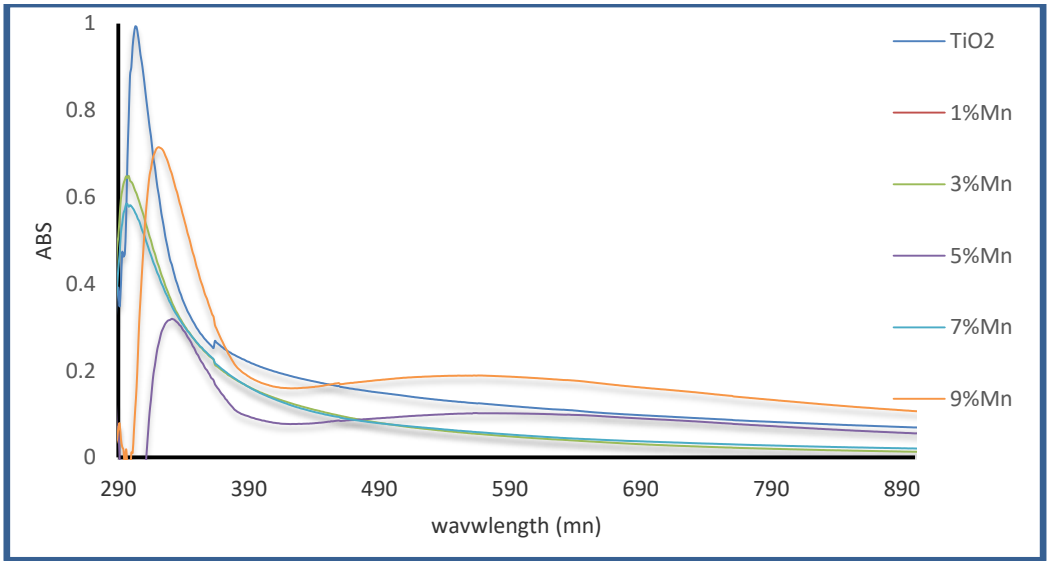

Fig.5: The pure and Mn-doped TiO_2 UV-Vis. spectral absorption curve.

4. Contact angle measurement

The hydrophilic properties were studied in this work. The self-cleaning operation of the thin films prepared at 500 ˚C was measured, the films were exposed to irradiance below 18 watts, the UV source with a range of (200-400) nm, the hydrophilicity of the samples was evaluated for TiO_2 and Mn-doped in three separate time periods. We also performed the calculation of the contact angle of the photographic images displayed in Figs.6-11, using the sessile projection method. Captured to assess the contact angles under air control, to differentiate between the advanced and receding contact angles. After storing the samples in darkness for ten days, the contact angle measurements for all the prepared samples were taken. As in Figure (a), the pure sample was the least contact angle, as it reached in 15 minutes to θ<10 UV rays, the surface of this sample was completely wet, and it can be seen that the hydrophilic in terms of the contact angle is related to the catalytic activity of the film where the angles are the smallest contact Responsible for more hydrophilicity, which is well consistent with the discovery of guan [26], According to the Wenzel equation, this element plays a more effective role in the extent of hydrophilicity [27], and the Table 4 shows the values of the contact angle of Wenzel equation, this values plays a more effective role in the extent determined by hydrophilicity.

$$Cos\theta' = rCos\theta \qquad (2)$$

where (θ') is the apparent contact angle and (r) is the surface roughness ratio between the actual surface area and the apparent surface area.

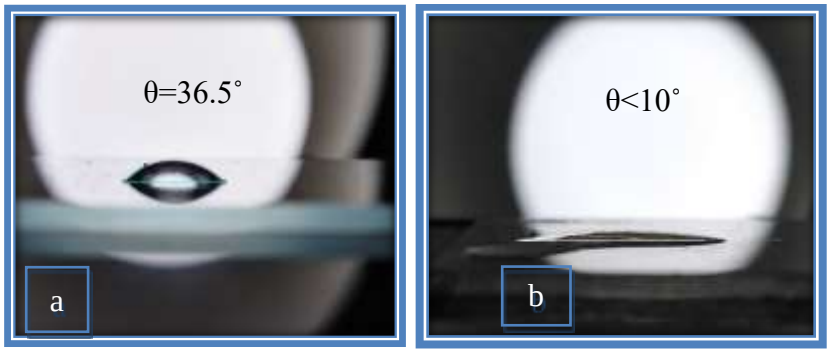

Fig .6: Images of water droplet on the sample pure TiO_2 (T): a- without UV irradiation, b- after15 min. of UV irradiation.

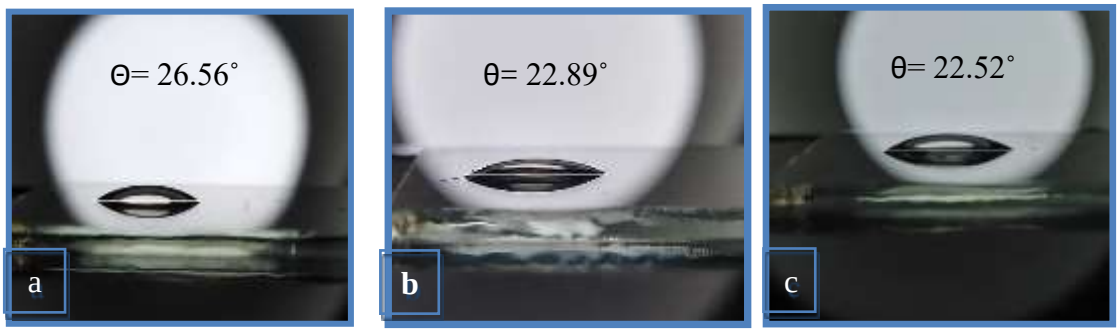

Fig.7a: Images of water droplet on the sample pure TiO_2 (Tm1): a-15min UV irradiation, b- after15 min. of UV irradiation c-an hour UV irradiation.

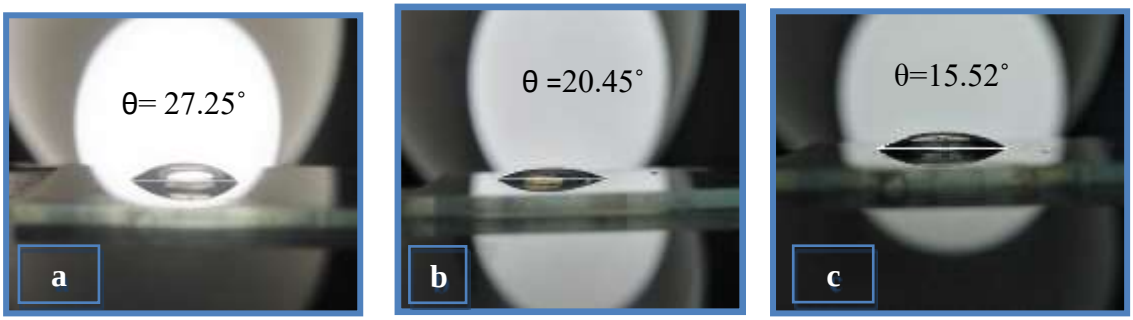

Fig.7b: Images of water droplet on the sample pure TiO_2 (Tm1): a-15min Vis irradiation, b- after15 min. of Vis irradiation c- an hour Vis irradiation.

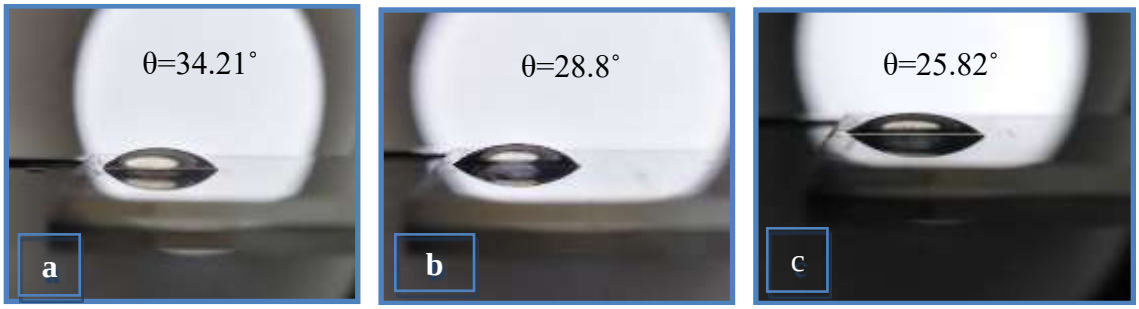

Fig.8a: Images of water droplet on the sample pure TiO_2 (Tm2): a-15min UV irradiation, b- after 15 min. of UV irradiation c -an hour UV irradiation.

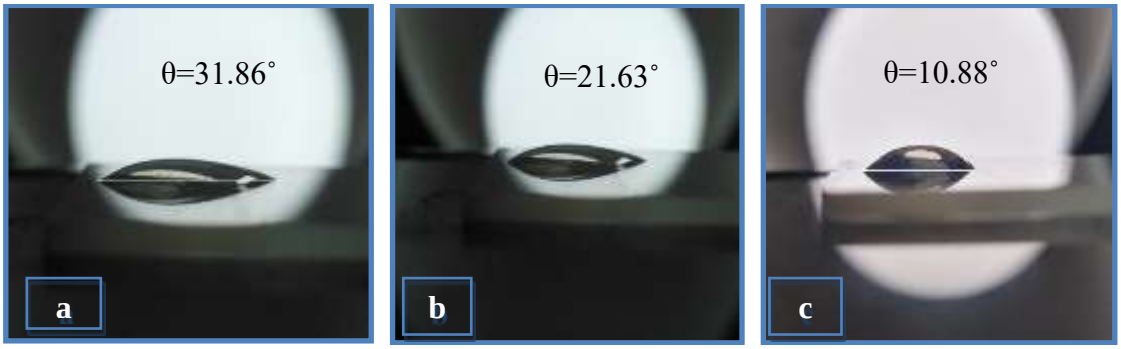

Fig8b: Images of water droplet on the sample pure TiO_2 (Tm2): a-15min Vis irradiation, b-after15 min. of Vis irradiation c- an hour Vis irradiation.

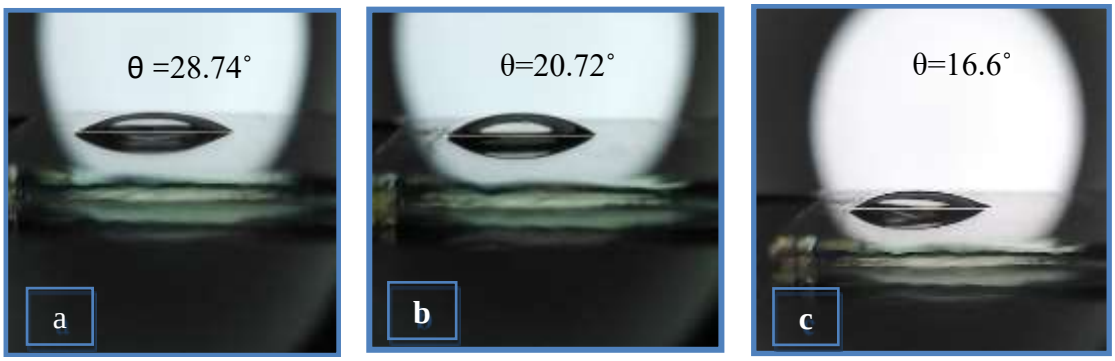

Fig.9a: Images of water droplet on the sample pure TiO_2 (Tm3): a-15min UV irradiation, b- after15 min. of UV irradiation c- an hour UV irradiation.

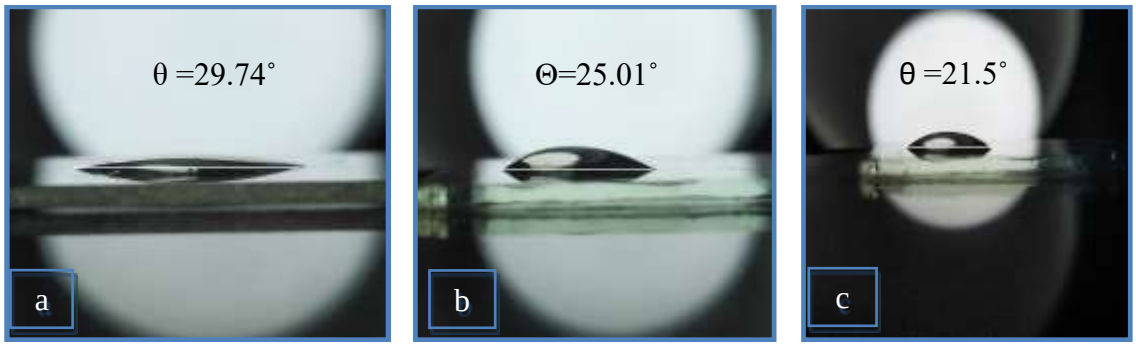

Fig.9b: Images of water droplet on the sample pure TiO2 (Tm3): a-15min Vis irradiation, b- after15 min. of Vis irradiation c- an hour Vis irradiation.

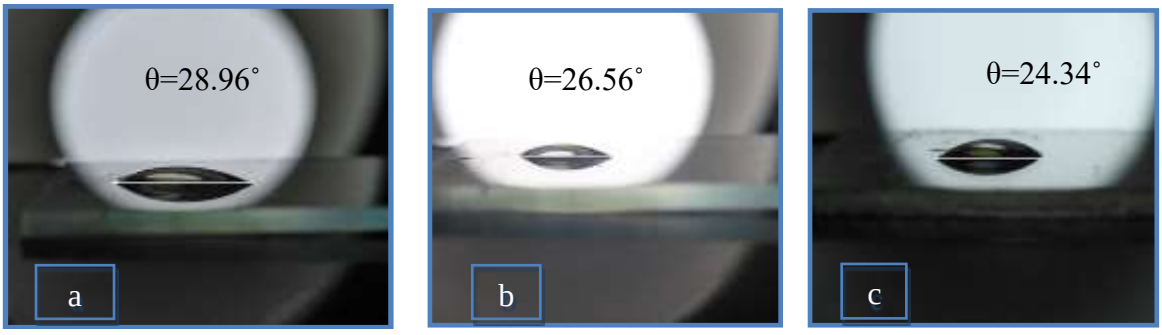

Fig.10a: Images of water droplet on the sample pure TiO_2 (Tm4): a-15min UV irradiation, b- after15 min. of UV irradiation c- an hour UV irradiation.

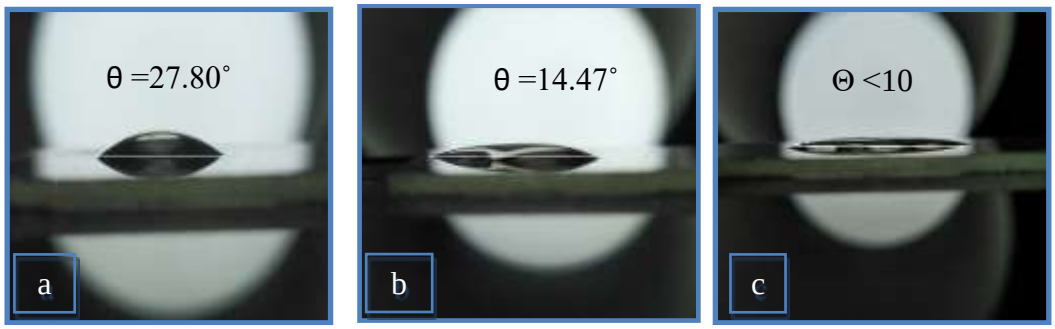

Fig.10b: Images of water droplet on the sample pure TiO_2 (Tm4): a-15min Vis irradiation, b- after15 min. of Vis irradiation c- an hour Vis irradiation.

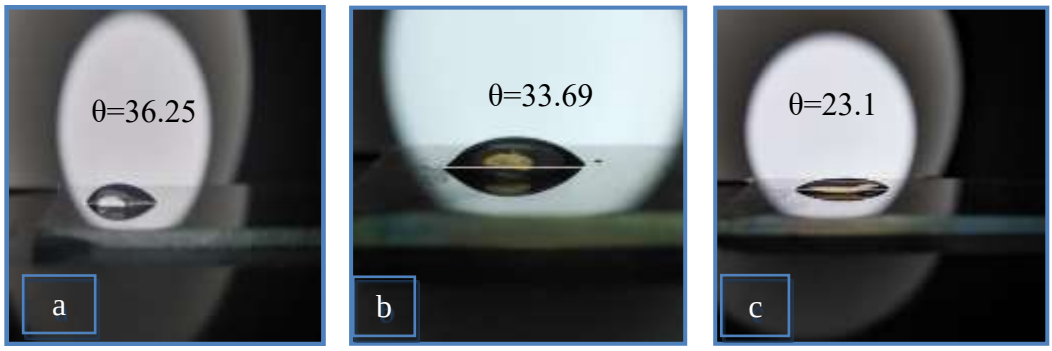

Fig.11a: Images of water droplet on the sample pure TiO_2 (Tm5): a-15min UV irradiation, b- after15 min. of Uv irradiation c- an hour UV irradiation.

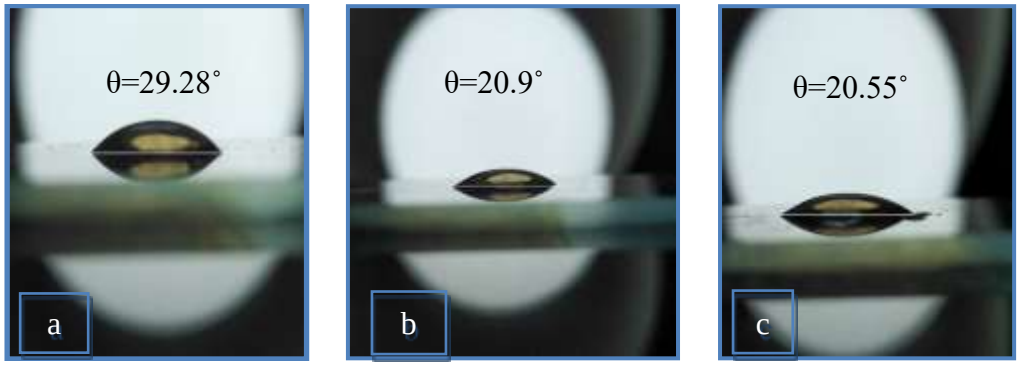

Fig.11b Images of water droplet on the sample pure TiO_2 (Tm5): a-15min Vis irradiation, b- after15 min. of Vis irradiation c- an hour Vis irradiation.

Table 3: Contact angle of Mn-doped TiO_2 all samples.

Samples	With Out θ'	UV-contact angle			Vis-contact angle		
		15min	30min	1h	15min	30mim	1h
Tm1	36.52	26.25˚	22.89˚	22.52˚	27.25˚	20.45˚	15.52˚
Tm2		34.21˚	28.81˚	25.82˚	31.86˚	21.63˚	10.88˚
Tm3		28.74˚	20.72˚	16.6˚	29.74˚	25.01˚	21.5˚
Tm4		28.96˚	26.56˚	24.34˚	27.80˚	14.47˚	8.1˚
Tm5		36.25˚	33.65˚	23.1˚	29.29˚	20.95˚	20.55˚

Conclusions

Pure TiO_2 and Mn-doped TiO_2 (1%, 3%, 5%, 7%, 9%) nanoparticles were synthesized pared successfully by sol-gel dip-coating, upon calcination of fixed 500 ˚C. The resulting products Characterized by X-ray diffraction (XRD), scanning electron microscopy (SEM), and absorption of UV-VIS. The XRD results showed anatase phase for the pure and Mn doped titanium samples with strong peak of (101) at 2θ=25 degree. The SEM images revealed the least particle size at 7% weight percentage, compared to the XRD results. Observed the red shift at the edge of absorption was achieved when increasing the manganese content, which led to a decrease in the indirect band gap from (3.2 - 2.55) eV, to allow for good absorption in the visible region. All these results illustrate that materials are suitable for photocatalytic applications, as well as self-cleaning, Under UV and visible light. Hydrophilic properties demonstrate (super hydrophilicity) where θ reaching less than 10˚ in 15 minutes.

Acknowledgement

The author's thanks all Molecular Laboratory group, University of Baghdad, College of Science, Department of Physics, for technical assistance during the research work.

References

[1] W. Y. Teoh, J. A. Scott, R. Amal, The Journal of Physical Chemistry Letters, 3, 5 (2012) 629-639.
[2] A. L. Linsebigler, G. Lu, Jr, J. T. Yates, Chemical Reviews, 95, 3 (1995) 735-758.
[3] S. Sakthivel & H. Kisch, Angewandte Chemi. International Edition, 42, 40 (2003) 4908-4911.
[4] M. R. Hoffmann, S. T. Martin, W. Choi, D. W. Bahnemann, Chemical Reviews, 95, 1 (1995) 69-96.
[5] A. Mills & S. K. Lee, A. Journal of Photochemistry and Photobiology A: Chemistry, 152, 1-3 (2002) 233-247.
[6] P. Zhong, W. Que, J. Chen, X. Hu, Journal of Power Sources, 210, (2012) 38-41.
[7] J. Sheng, L. Hu, W. Li, H. Tian, S. Dai, Solar Energy, 85, 11 (2011) 697-2703.
[8] G. Shemer, Y. Paz, International Journal of Photoenergy, 2011 (2011) 1-7.
[9] M. Montazer, S. Seifollahzadeh, Photochemistry and Photobiology, 87, 4 (2011) 877-883.
[10] A. Nakaruk, D. Ragazzon, C. C. Sorrell, Thin Solid Films, 518, 14 (2010) 3735-3742.
[11] D. J. Kim, S. H. Hahn, S. H. Oh, E. J. Kim, Materials Letters, 57, 2 (2002) 355-360.
[12] K. Liu, M. Cao, A. Fujishima, L. Jiang, Chemical Reviews, 114, 19 (2014) 10044-10094.
[13] H. Yaghoubi, N., Taghavinia, E. K. Alamdari, Surface and Coatings Technology, 204, 9-10 (2010) 1562-1568.
[14] I. P. Parkin, & R. G. Palgrave, Journal of Materials Chemistry, 15, 17 (2005) 1689-169).
[15] F. Bondioli, R. Taurino, A. M. Ferrari, Journal of Colloid and Interface Science, 334, 2 (2009) 195-201.
[16] W. Li, & A. Amirfazli, Advance in Colloid and Interface Science, 132, 2 (2007) 51-68.
[17] W. Barthlott & C. Neinhuis, Planta, 202, 1 (1997) 1-8.

[18] S. Nishimoto & B. Bhushan, RSC Adv., 3, 3 (2013) 671-690.
[19] D. Nanda, A. Sahoo, A. Kumar, B. Bhushan, Journal of Colloid and Interface Science, 535 (2019) 50-57.
[20] N. Zhao, Z. Wang, C. Cai, H. Shen, F. Liang, D. Wang, X. Liu, Bioinspired. Advanced Materials, 26, 41 (2014) 6994-7017.
[21] A. H. Hasan, F. H. Ali, B. T. Chiad, Iraqi J. of Physics, 16, 39 (2018) (64-70).
[22] F. H. Ali, "Modification of TiO_2 Photocatalytic Sensitivity from UV to Visible Light", PhD Thesis, University of Baghdad, (2015).
[23] S. N. R. Inturi, T. Boningari, M. Suidan, P. G. Smirniotis, Applied Catalysis B: Environmental, 144 (2014) 333-342.
[24] Q. R. Deng, X. H. Xia, M. L. Guo, Y. Gao, G. Shao, Materials Letters, 65, 13 (2011) 2051-2054.
[25] K. Guan, Surface and Coatings Technology, 191, 2-3 (2005) 155-160.
[26] R. N. Wenzel, the Journal of Physical Chemistry, 53, 9 (1949) 1466-1467.